https://doi.org/10.5194/egusphere-2025-268
Preprint. Discussion started: 26 March 2025

Towards an integrated inventory of anthropogenic emissions for China

Yijuan Zhang[1,2], Guy Brasseur[2], Maria Kanakidou[1,3,4], Claire Granier[5,6], Nikos Daskalakis[1], Alexandros Panagiotis Poulidis[1], Kun Qu[1], and Mihalis Vrekoussis[1,7,8]

[1]Laboratory for Modeling and Observation of the Earth System (LAMOS), Institute of Environmental Physics (IUP), University of Bremen, Bremen, Germany
[2]Environmental Modelling Group, Max Planck Institute for Meteorology, Hamburg, Germany
[3]Environmental Chemical Processes Laboratory(ECPL), Chemistry Dept., University of Crete, Greece
[4]Center of Studies on Air quality and Climate Change (CSTACC), ICE-HT/FORTH, Patras, Greece
[5]Laboratoire d'Aerologie, Toulouse, France
[6]NOAA/CSL-CIRES/University of Colorado, Boulder, CO, USA
[7]Climate and Atmosphere Research Center (CARE-C), The Cyprus Institute, Cyprus
[8]Center of Marine Environmental Sciences (MARUM), University of Bremen, Bremen, Germany

Correspondence: Yijuan Zhang (yijuan.zhang@outlook.com), Guy Brasseur (guy.brasseur@mpimet.mpg.de) and Mihalis Vrekoussis (mvrekous@uni-bremen.de)

Abstract.

Despite ongoing efforts to reduce pollution, persistent ozone pollution in China remains a public health concern. To better understand the causes of ozone pollution in China and to assess and evaluate the effectiveness of past, current, and planned targeted pollution control strategies, estimates of the amounts of pollutants emitted from various sources are needed. To this end, we have developed harmonized and integrated anthropogenic emission inventories for China, incorporating information from the existing national inventory for mainland China (MEIC) and three global inventories (CEDS, CAMS, HTAP) to cover areas outside of China. The newly developed China INtegrated Emission Inventory (CINEI) includes emissions in China from sectors currently omitted from the MEIC (ships, aviation, waste, and agriculture) that we incorporate from the global inventories. To ensure harmonized emissions data, we performed mapping between different inventories, a process used to achieve consistency between sectors, spatial resolution, and speciation of non-methane volatile organic compounds (NMVOCs). These harmonized and integrated inventories for China were used to drive WRF-Chem simulations for January (winter) and July 2017 (summer). Through a detailed evaluation of model results against available observations, we show that while the direct use of global inventories alone can lead to severe over- or underestimation of pollutant mixing ratios, CINEI inventories perform satisfactorily in simulating ozone (12% in summer and 43% in winter normalized mean bias) and its precursors, including nitrogen dioxide (NO_2, -0.5% in summer and 40% in winter) and carbon monoxide (CO, -50% in both seasons). Based on the comparison and modeling of this study, valuable insights into the spatio-temporal variability of ozone and the subsequent design of future ozone mitigation strategies in China were provided.

https://doi.org/10.5194/egusphere-2025-268
Preprint. Discussion started: 26 March 2025

1 Introduction

China's air quality has improved rapidly since 2013 in response to the implementation of mitigation strategies (Zhang et al., 2019). Concentrations of particulate matter ($PM_{2.5}$) and primary pollutants (e.g., nitrogen oxides, sulfur dioxide, and carbon monoxide) have decreased (Wang et al., 2019; Liu and Wang, 2020; Wang et al., 2023). However, ground-level ozone pollution remains severe. In 2017, the population-weighted exposure-averaged mixing ratio of ozone in China reached 68.2 parts per billion by volume (ppbv) (Yin et al., 2020), exceeding the World Health Organization (WHO) air quality standard of 50 ppbv (Lyu et al., 2023; World Health Organization, 2021). Ground-level ozone is a secondary pollutant formed in complex photochemical reaction chains from its precursors, including nitrogen oxides (NO_x = NO + NO_2), carbon monoxide (CO), and non-methane volatile organic compounds (NMVOCs). Therefore, the amounts of emitted precursors based on different anthropogenic emission inventories may lead to different estimates of ozone mixing ratios. To investigate near-surface ozone pollution, its multi-year changes, and the effects of sectoral emissions of precursors on ozone distribution over China, it is essential to accurately represent the amount and spatiotemporal variations of anthropogenic emissions of ozone precursors in emission inventories (Li et al., 2017; Chang et al., 2022; Smith et al., 2022; Monks et al., 2015). Therefore, emission inventories are essential to provide the information needed to formulate effective strategies to further improve air quality (Hoesly et al., 2018).

Over the past decade, anthropogenic emissions in China have undergone rapid changes due to air pollution reduction strategies (Fig. S1a). In particular, since 2013 during the implementation of 12th Five-Year Plan period (12^{th} Five-Year Plan, 2011), there were significant reductions in anthropogenic emissions of -27% for NOx and -17% for CO (Zheng et al., 2018). These reductions were due to measures such as setting ultra-low emission standards for vehicles and factories, improving air quality control technologies, and phasing out high-emitting factories (Li et al., 2017; Lu et al., 2020). After 2010, CO and NO_2 mixing ratios gradually fell below the WHO standards of 0.4 parts per million by volume (ppmv) for CO and 20 ppbv for NO_2 (Text S1 and Fig. S1b). Despite these significant improvements in air quality (Zhang et al., 2019), there is growing concern about unintended increases in ozone levels (Li et al., 2019; Lu et al., 2020)., which may result from the co-effects of reduced NO_x emissions and increased NMVOC emissions (Li et al., 2019). As a result, specific strategies targeting NMVOC emissions were introduced in 2015, especially in the petrochemical and organic chemical industries. Despite these measures, maximum daily 8-h average ozone levels remained high in 2022 (Fig. S1b) and frequently exceeded the WHO thresholds during the warm season (April to October, Fig. S1b). Although total NMVOC emissions have decreased in China, some studies attribute the observed increase in ozone over the past decade to the increasing contribution of anthropogenic NMVOC emissions, especially aromatics, alkenes, and oxygenated VOCs (OVOCs), mainly from the petrochemical industry and solvent use, to the total NMVOCs (Li et al., 2014; Zhang et al., 2020, 2021; McDonald et al., 2018). In order to investigate the drivers of recent changes in ozone pollution in China, it is crucial to develop accurate emission inventories that reflect policy-driven changes in anthropogenic emissions.

However, existing anthropogenic emission inventories encounter discrepancies in sectoral emission (Solazzo et al., 2021). The discrepancy raises concerns about their accuracy and reliability (Crippa et al., 2021; McDonald et al., 2018). Anthro-

https://doi.org/10.5194/egusphere-2025-268
Preprint. Discussion started: 26 March 2025

pogenic emission inventories are typically constructed in a bottom-up manner, with sectoral emissions quantified using activity data and emission factors (Solazzo et al., 2021). Activity data are mainly derived from official statistics (see Text S2 for details). Emission factors provide the amount of emissions released per activity (Text S2). To obtain gridded emissions with specified NMVOC speciation and high spatiotemporal resolution, we need more detailed NMVOC speciation profiles, temporal profiles, and associated source proxies to distribute emissions in space. Discrepancies in anthropogenic emissions between global, regional, and national emission inventories in describing emissions within a region can be attributed to differences in all of the aforementioned data. Regional and national inventories often use updated and more localized activity data, emission factors, and spatial proxies (Text S3). Thus, they are likely to better quantify emissions within the region or nation of interest and better describe their multi-year changes and spatial distributions compared to global inventories. However, national inventories that are limited to the region of interest do not capture air pollutants transported from regions outside the national territory. In addition, some emission sectors may be missing. The use of different NMVOC speciation profiles can also lead to differences in ozone simulations, and its influence must be considered (Rowlinson et al., 2024).

The integration of local or regional emissions into larger scale emissions, called MOSAIC emissions (Li et al., 2024b), can improve the accuracy of emission inventories in reproducing the amounts and variations of emissions. This approach has been applied in many studies, including the integration of metropolitan-regional emissions into national emissions (Wu et al., 2024), national emissions into continental emissions (Li et al., 2024a), and continental emissions into global emissions (Crippa et al., 2023). The use of these integrated emission inventories in chemical transport models (CTMs) leads to improved model performance in reproducing pollutant concentrations. A comprehensive comparison between the results of the simulations and the observations can demonstrate the improvements achieved in pollutant simulations.

In this study, we aim to construct a comprehensive anthropogenic emissions inventory for China (CINEI) by integrating the emissions data from mainland China's inventory (Multi-resolution Emission Inventory model for China, MEIC) with various global emission inventories within our integrated (harmonized) emissions system (Fig. 1a). Our goal is to develop an emission inventory that integrates emissions from all sectors, well-defined localized NMVOC speciation, and provides a spatial distribution of emissions consistent with the framework of global emission inventories. The processing method is presented in section 2.2. We discuss the results of CINEI emissions in terms of emission sectors (Section 3.1), NMVOC speciation (Section 3.1), and spatial distributions (Section 3.1), and compare them with existing emission inventories. In order to assess the reliability of the new CINEI inventory, we performed numerical WRF-Chem regional experiments based on CINEI, MEIC (harmonized inventories) and three global inventories, as described in Section 3.1. The model performance is evaluated and discussed in Section 3.1. Based on the discussion of this study, we make recommendations for future emissions and modeling studies (Section 4).

https://doi.org/10.5194/egusphere-2025-268
Preprint. Discussion started: 26 March 2025

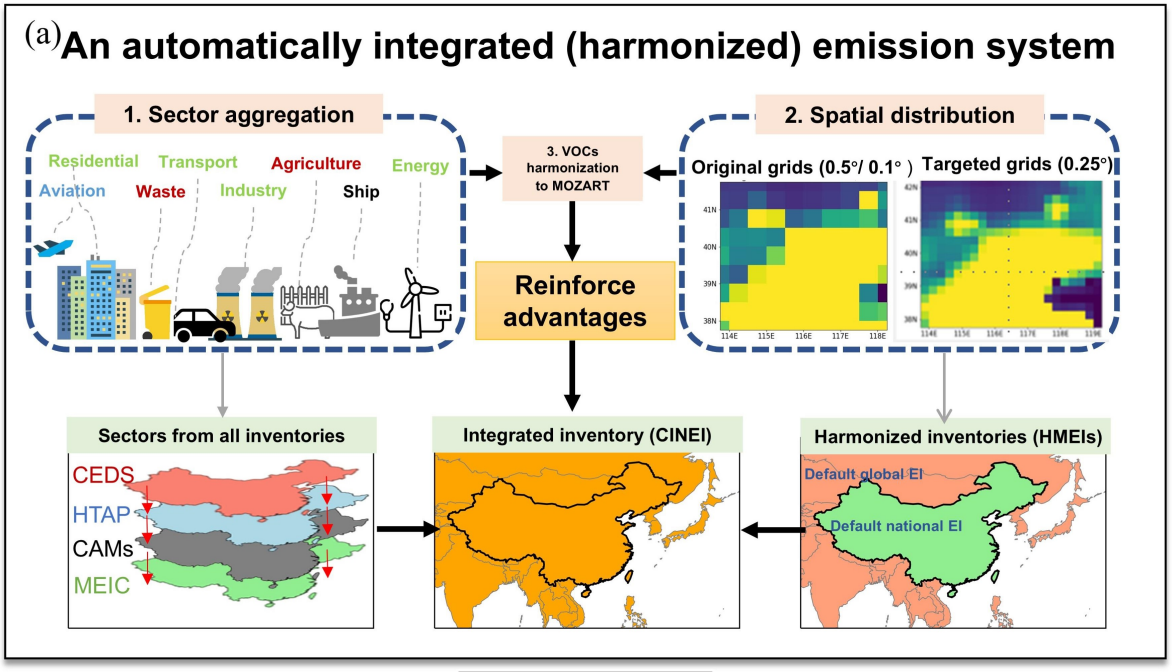

Validation

(b) **WRF-Chem & Observation**

Experiments based on different inventories			
➢ Harmonized inventories (HMEIs)	HM_CAMs	HM_CEDS	HM_HTAP
➢ Global inventories	CAMs	CEDS	HTAP
➢ Integrated (CINEI)	Integrated		

Figure 1. Representation of the framework of an integrated (harmonized) emission inventory system (top two panels) and its evaluation scheme (bottom panel). Figure 1a illustrates the procedure for the construction of the harmonized and integrated (CINEI) emission inventories, which is explained in Section 2.2. Figure 1b shows the WRF-Chem experiments performed to validate the emission inventories, with detailed explanations in Section 2.2.

https://doi.org/10.5194/egusphere-2025-268
Preprint. Discussion started: 26 March 2025

2 Methodology

2.1 Selection of anthropogenic emission inventories

For the purpose of developing the CINEI, we selected emission inventories based on the following criteria:

- **Data availability**: We prioritized emission inventories that are easily accessible and widely used by the scientific community.
- **Multi-annual coverage**: The anthropogenic emission inventories need to span multiple years and accurately reproduce emission changes within the recent 10-12 years.
- **High temporal resolution**: We selected emission inventories with monthly or higher temporal resolution to account for seasonal variations.
- **Gridded emissions**: Gridded emissions are essential for simulation using CTM.
- **NMVOC speciation**: NMVOCs is tropospheric ozone precursors and as such their they are crucial for ozone simulations in CTM and understanding their potential impact on ozone formation, hence their emissions need to be adequately speciated.
- **Avoiding data duplication and unnecessary integrations**: As some regional inventories are included in global inventories, only global inventories were selected for this study.

Based on the above considerations, we selected four anthropogenic emission inventories (Table 1) that include one regional (national) and three global emission inventories. These are:

1. **The Multi-resolution Emission Inventory for China (MEIC version 1.4)**: MEIC is a national inventory for mainland China developed by Tsinghua University and updated to the year 2020 (Zheng et al., 2018, 2021a). Due to the 22 emission sectors provided in the newer version 1.4 (released in 2023), we use MEICv1.4 to improve sectoral comparisons in our study. The previous version, MEICv1.3, has been widely used in a number of research studies to date (Liu and Wang, 2020; Wang et al., 2024). We also provide comparisons of emission amounts (NO_x, CO, and NMVOCs) between MEICv1.3 and MEICv1.4 in Fig. S2. MEICv1.4 data used in this study are provided in Zenodo (Zhang, 2025b). Absolute differences of annual averages (MEICv1.3 values minus latest MEICv1.4 values over MEICv1.3 values) were calculated and then expressed as percentages with respect to the annual average emissions in the more recent emission inventory. The differences in total pollutant emissions in China between the two versions were found to be less than 5%, and differences between other versions of inventories follow the same calculation.
2. **The Community Emissions Data System (CEDS, version 2021)**: This is a global emission inventory for the Coupled Model Intercomparison Project Phase 6 (CMIP6) (Hoesly et al., 2018; Feng et al., 2020; Smith et al., 2022). CEDSv2021 provides detailed descriptions of emission sectors and IPCC sector codes, which facilitates inter-comparison of sectoral

https://doi.org/10.5194/egusphere-2025-268
Preprint. Discussion started: 26 March 2025

emissions (Hoesly et al., 2024). Comparisons between CEDSv2021 and the previous version, CEDSv2019, suggest that there are only slight differences (< 3%) in the emissions of ozone precursors in China (Fig. S4), therefore CEDSv2019 is not included in further analysis.

3. **The Copernicus Atmosphere Monitoring Service emissions (CAMS, version 5.3)**: This dataset is based on the Emission Database for Global Atmospheric Research (EDGAR version 5) until 2018, and projected to 2022 by using the linear slopes of CEDS sectoral emissions from 2015 to 2019 (Granier et al., 2019; Doumbia et al., 2021; Soulie et al., 2023). We also compared pollutant emissions in China in CAMSv5.3 and the latest version of EDGAR, EDGAR v6.1 (Fig. S3). CAMSv5.3 data used in this study are provided in Zenodo (Zhang, 2025b). Results indicate the similarity between the two emission inventories, with differences ranging from 4 to 7% for total annual emission for China, from 2008 to 2020. Thus, EDGAR v6.1 was not selected for this study.

4. **Hemispheric Transport of Air Pollution (HTAP, version 3)**: HTAP is a newly published global emissions inventory (2023) that incorporates the Regional Emission Inventory of Asia (REAS, version 3.2.1) for pollutant emissions in East, Southeast, and South Asia (including China) (Kurokawa and Ohara, 2020; Crippa et al., 2023). HTAPv3 includes more comprehensive sectoral emissions than REASv3.2.1, including domestic and international aviation and shipping, waste emissions, and agricultural waste burning from EDGAR (Monica, 2023). HTAPv3 reports higher emissions than REASv3.2.1, by 2.5 Tg (8.8%) for NO_x and by 2.5 Tg (8.7%) for NMVOC, while the difference in CO emissions between the two inventories is less than 0.5% (Fig. S5 and Text S4). We retained the HTAP inventory in our study because it is consistent with the framework of global emission inventories.

Table 1. List of emission inventories considered for integrated inventory

Acronym	Version	Period	Spatial Resolution	Website	Last Access Time
MEIC	1.4	2008 to 2020	0.25°	http://meicmodel.org.cn/?page_id=1772&lang=en	March 2025
CAMS	5.3	2008 to 2020	0.1°	https://eccad.sedoo.fr/#/metadata/479	May 2024
CEDS	2021	2008 to 2019	0.5°	https://data.pnnl.gov/dataset/CEDS-4-21-21	May 2024
HTAP	3	2008 to 2018	0.1°	https://edgar.jrc.ec.europa.eu/dataset_htap_v3	May 2024

2.2 Harmonizing and integrating emission inventories

In order to improve comparability and build on the strengths of national (MEIC) and global emission inventories, our goal was to develop an integrated emissions was to develop an integrated emission inventory for China (CINEI) based on harmonized emission inventories, but with emissions from all activity sectors in China following the IPCC definitions of emission sectors and updated NMVOC speciation with observation-based, localized profiles. To do this, we harmonized the emission inventories by unifying the definition of emission sectors, spatial resolutions, and NMVOC speciation between the MEIC and global

https://doi.org/10.5194/egusphere-2025-268
Preprint. Discussion started: 26 March 2025

emissions. The framework for creating the harmonized CINEI is shown in Fig. 1a, and the Python code for this processing can be accessed on the Zenodo website (https://zenodo.org/records/15000795) and archived by Zhang (2025a). Further details are provided below:

[Step 1 - Sectoral mapping]: Harmonizing emission sectors between the national and global emission inventories. The classification of emission sectors often differs between different emission inventories. To compare sectoral emissions and harmonize emission sectors, we first need to use emission sector mapping tables to establish the correspondence between the emission sector definitions in the selected emission inventories and the standard sub-sector codes of the IPCC (Intergovernmental Panel on Climate Change; IPCC, 2006), as shown in Fig. S6. The correspodance of emission sectors is based on their definitions for each inventory, which are collected through extensive literature and data documentation on the official website (Granier et al., 2019; Li et al., 2024b; Crippa et al., 2023). Eight sectors are defined in the harmonized and integrated emission inventories, including:

1. Transportation: Emissions from both road and non-road transport. Emissions are quantified based on fuel consumption, and vehicles contributing to such emissions include heavy and light trucks, rail vehicles, passenger cars and motorcycles, etc. Emissions from international shipping and aviation are excluded from this emission sector.
2. Residential: Emissions from small-scale residential and commercial activities, including heating, cooling, lighting and cooking, as well as auxiliary engines used in houses, commercial buildings, service institutes, etc.
3. Power: Emissions from electricity generation, commonly driven by large-scale intensive fuel combustion. The incineration of waste in waste-to-energy plants is also included.
4. Industry: Emissions from by-product industrial processes, including emissions from solvent volatilization, cement, iron and steel production, fugitive emissions, refinery emissions and other fuel-related emissions.
5. Agriculture: Emissions from agricultural soil, manure management, cultivation, and agriculture waste burning. Agriculture waste burning includes straw burning, and excludes savannah burning (Crippa et al., 2023). Besides, transportation emissions due to the usage of agricultural vehicles (such as fishing boats) are also included here.
6. Waste: Emissions related to solid waste disposal and wastewater treatment.
7. Aviation: Emissions from aviation activities, including the take-off, cruising and landing of aircraft.
8. Ships: Emissions from shipping activities on both oceans and inland waterways.

Table 2 lists the data sources for CINEI sectoral emissions and the missing sectors in the existing inventories. By following the IPCC sector definitions, we were able to identify sectors that were omitted from certain emission inventories (Fig. S6). For CINEI, we kept the emissions for the four existing sectors (transportation, residential, industry, and energy) used in the MEIC, and for the four missing sectors, we added emissions from various global emission inventories for the four missing sectors. Specifically, we used aviation and domestic shipping emissions from HTAP and ocean shipping emissions from CAMS. For

https://doi.org/10.5194/egusphere-2025-268
Preprint. Discussion started: 26 March 2025

the agriculture and waste sectors, we used the corresponding data from CEDS. In particular, agricultural emissions in the MEIC only consider NH_3. Therefore, agricultural emissions of all species from the CEDS were used in the CINEI. The above processing ensures comprehensive sectoral coverage and consistency between national and global emission inventories.

https://doi.org/10.5194/egusphere-2025-268
Preprint. Discussion started: 26 March 2025

Table 2. Data sources of CINEI sectoral emissions and mapping with global emission inventories

Sectors	CINEI Data Source	If provided by existing inventories			
		MEIC	CEDS*	CAMS	HTAP*
Power	MEICv1.4	√	√	√**	√
Industry	MEICv1.4	√	√	√**	√
Residential	MEICv1.4	√	√	√	√
Aviation	HTAPv3	missing	missing	missing	√
Transportation	MEICv1.4	√	√	√	√
International Ships	CAMSv5.3	missing	√	√	√
Domestic Ships	HTAPv3	missing	missing	√	√
Agriculture	HTAPv3	√**	√	√	√
Waste	CEDSv2021	missing	√	√	√**

*As emissions from HTAP and CEDS are not extended to 2020, we use a linear regression of the emissions from 2008 to 2018 (2019) for HTAP (CEDS) and extrapolate to 2020 for CINEI.

** indicates that the emissions inventory provides parts of the sectoral emissions, but misses some subsectors suggested by the IPCC report. Details on IPCC subsectors and comparison to each inventory are listed in Fig. S6.

We also analyzed the changes in ozone precursor emissions in China. The trend in emissions from a sector x is calculated for the studied period of 2008 to 2020 using the Equation (1).

$$\mathrm{T}_x = \frac{\mathrm{E}_{x,2008}}{\sum_n^{k=1} \mathrm{E}_{k,2008}} \times \left| \frac{\mathrm{E}_{x,2020} - \mathrm{E}_{x,2008}}{\mathrm{E}_{x,2008}} - \frac{\sum_n^{k=1} \mathrm{E}_{k,2020} - \sum_n^{k=1} \mathrm{E}_{k,2008}}{\sum_n^{k=1} \mathrm{E}_{k,2008}} \right|, \quad (1)$$

where:

- T_x is the relative changes of emissions from the emission sector x in the end years for global inventories that stops at 2018 for HTAP and 2019 for CEDS, we extrapolate the data to year of 2020 through linear regression,
- $\frac{E_{x,2008}}{\sum_{k=1}^{n} E_{k,2008}}$ is the relative changes of emissions from the emission sector x in the end years for global inventories that stops at 2018 for HTAP and 2019 for CEDS, we extrapolate the data to year of 2020 through linear regression,
- $\frac{E_{x,2020}-E_{x,2008}}{E_{x,2008}}$ gives the relative change in emission from sector x from 2008 to 2020,
- $\frac{\sum_{k=1}^{n} E_{k,2020}-\sum_{k=1}^{n} E_{k,2008}}{\sum_{k=1}^{n} E_{k,2008}}$ gives the relative change in total emissions from 2008 to 2020.

We defined key sectors as those with an obvious influence on changes in total national emissions of a pollutant. We identified key sectors based on the following two criteria: (1) they show a clear increasing or decreasing trend in line with total emissions; (2) the total contributions of the key sectors can explain more than 95% of the total emissions changes. We have adopted this calculation from Intergovernmental Panel on Climate Change (IPCC) (2006).

https://doi.org/10.5194/egusphere-2025-268
Preprint. Discussion started: 26 March 2025

[Step 2 – Uniform spatial resolution]: Re-gridding emission data to the same spatial resolution. The global inventories under consideration have different horizontal resolutions, ranging from 0.1° to 0.5° in both longitude and latitude. To ensure a consistent integration, we need to align their resolutions. Therefore, to match the resolution of the MEIC, we spatially interpolated all global inventory data to the grid coordinate with a resolution of 0.25° × 0.25° (latitude x longitude). We used 'Conservative' algorithms for the adjustment, which ensures that the quantity of emissions in the new grids does not change compared to that in the old grids. The emissions in mass in the new grid cell k (denoted as E_k) are quantified by Equation (2),

$$\mathrm{E}_k = \int\int_{A_k} e(r)dA, \tag{2}$$

where e(r) is the emission density in the old grid cell that intersects with this new grid, and A_k indicates the areas of intersections between two grids (Dukowicz, 1984). These integrals must be calculated for all cells of the new mesh.

[Step 3 – NMVOC speciation mapping]: Aligning NMVOC emissions in all emission inventories to the same speciation.

NMVOC emissions are assigned different speciations in different inventories. NMVOC speciation in regional and national inventories (e.g., MEIC and REAS) often follows chemical mechanisms widely used in models, such as the Carbon Bond Mechanism (CBM) (Gery et al., 1989), the Regional Acid Deposition Model gas-phase chemical mechanism (RADM) (Iacono et al., 2008), and the State Air Pollution Research Center (SAPRC) (Carter, 2015). Regional inventories often speciate NMVOC species according to the Model for Ozone and Related chemical Tracers mechanism (MOZART) (Li et al., 2014; Huang et al., 2017). We also assumed MOZART speciation for the integrated inventory (Table S10). This facilitates comparison of speciated NMVOC emissions with global inventories and application in global models, because the MOZART speciation is also used in global inventories and global CTMs (Lamarque et al., 2010; Huang et al., 2017; Emmons et al., 2020). To perform the integration of emissions of specific NMVOC species and to meet the requirements of simulations by CTMs, it is essential to make the NMVOC speciation in different emission inventories consistent. For harmonized inventories, we applied a mapping table (Table S3) to align the MEIC NMVOC lumped species categories with those in the global inventories, and the MOZART speciation is applied to NMVOC emissions in all inventories after mapping. For the CINEI, we updated the NMVOC speciation by applying recently reported localized source profiles and lumped NMVOC emissions following the NMVOC categories in the MOZART mechanism (Emmons et al., 2020). Total NMVOC emissions from different sectors were assigned to more than 80 specific VOC species based on NMVOC speciation profiles reported by Mo et al. (2016) and Sha et al. (2021) (details in Table S4 and Table S10). These profiles describe well the recent speciation of NMVOC emissions in China based on representative measurements (Li et al., 2014). In order to evaluate and compare the impact of different NMVOC species on ozone formation, ozone formation potentials (OFPs) are calculated in this study. For the NMVOC species j, its OFP value is calculated by Equation (3):

https://doi.org/10.5194/egusphere-2025-268
Preprint. Discussion started: 26 March 2025

$$\mathrm{OFP}(j) = \mathrm{EVOC}(j) \times MIR(j), \quad (3)$$

where EVOC(j) is the emissions of j, and MIR(j) is the maximum incremental reactivity of j, defined as the potential maximum ozone production per consumption of j under high-NO_x conditions (Carter, 1994). The MIR values used in this study were derived from Carter (2015) and are listed in Table S5. The MIR indicates the amount of ozone growth as the incremental emission of NMVOC species increases, and is unitless. Therefore, the unit of OFPs should be mass based and here we use Tg-O_3.

[Step 4 – Emissions' harmonization and integration]: Spatial harmonization and integration of emissions by species and sector. In the previous three steps, the selected inventories (MEIC, CEDS, CAMS, HTAP) are transformed into new ones with consistent sector types, spatial resolutions, and NMVOC speciation (MOZART). This step harmonizes and integrates the national and global inventories and improves the compatibility of the integrated inventory with the chemical mechanism of the CTM. We focus on anthropogenic pollutant emissions in East Asia (70.125°E to 149.875°E and 10.125°N to 59.875°N), which is gridded in 320×200 grids. National and global inventories in this area are combined to produce Harmonized Emission Inventories (HMEI) and CINEI, the details of which are presented below:

- **Harmonized emission inventories (HMEI):** In these inventories, anthropogenic emissions within Mainland China are derived from the standard Chinese national inventories, MEIC and those outside of China are from the global emission inventories. Based on the type of global inventory used in the processing, three harmonized global emission inventories were created: HM_CAMS (harmonized MEIC with the CAMS global inventory), HM_CEDS (CEDS), and HM_HTAP (HTAP) when using MEIC.

- **Integrated emission inventory (CINEI):** Based on the harmonized emission inventories, CINEI also includes all emission sectors and updated NMVOC emissions speciated according to the MOZART chemical scheme (Zhang et al., 2025). As mentioned above, emissions from four sectors, including ships, waste, aviation and agriculture, are missing in the MEIC. In the CINEI, emissions from these missing sectors in China are derived from the global emission inventories as explained in Step 1 and shown in Table 2.

To consolidate the data fusion from national to global emission inventories at spatial scales, we calculated the Monte Carlo uncertainty for sectoral emissions for the global inventory (CEDS) and the regional CINEI (Lee et al., 2024). We randomly select 10000 samples from 64000 values (200×320), calculate the standard deviation of the samples, and repeat this step 1000 times until the standard deviation does not change. We use the standard deviation to represent Monte Carlo uncertainties, and if the standard deviations of the global and CINEI inventories are of the same magnitude, we assume that the data fusion is reliable (Heuvelink and Brus, 2009).

https://doi.org/10.5194/egusphere-2025-268
Preprint. Discussion started: 26 March 2025

2.3 Evaluating emission inventories Using WRF-Chem Model

To evaluate the performance of the harmonized and CINEI inventories, we used the Weather Research and Forecasting model with Chemistry (WRF-Chem, version 4.3.2; Skamarock et al. (2019); WRF Model Development Team (2025)) to run simulations for our region of interest with different inputs of anthropogenic emissions and compared the model results with measurements of ozone (O_3), carbon monoxide (CO), and nitrogen dioxide (NO_2). We performed simulations using each of the three global emission inventories (CAMS, CEDS, HTAP), three harmonized inventories (HM_CAMS, HM_CEDS, HM_HTAP), and CINEI (Fig. 1b), and for two different simulation periods, January (representing winter) and July (representing summer) 2017.

We used the same model setups for all experiments (Table S6). Specifically, we set up two unidirectionally nested simulation domains with spatial resolutions of $36\,\mathrm{km} \times 36\,\mathrm{km}$ and $12\,\mathrm{km} \times 12\,\mathrm{km}$ (Fig. 2). Specifically, the inner domain includes the major populated areas of eastern China. The domain has a dense network of air quality monitoring sites (Fig. 2) and meteorological monitoring sites (Fig. S7). The chemical initial and boundary conditions for the outer domain were derived from the 6-hourly output of the CAM-chem model (Lamarque et al., 2010), while for the inner domain they were extracted from the results of the simulation in the outer domain. MOZART (Emmons et al., 2020) was used to simulate gas-phase chemistry and reactions, and MOSAIC (MOdel for Simulating Aerosol Interactions and Chemistry; (Hodzic and Knote, 2014)) was set as the aerosol scheme. Biomass combustion emissions were taken from the FINN (Fire INventory from NCAR, version 1.5) inventory (Wiedinmyer et al., 2011), and biogenic emissions are estimated using the Model of Emissions of Gases and Aerosols from Nature (MEGAN, version 2.1) (Guenther et al., 2012). We set the spin-up time to 6 days before the study periods to avoid the influence of imbalanced chemical initial conditions on the simulation results.

To evaluate the model performance across all experiments, we compared the modeled hourly averaged mixing ratios of O_3, CO, and NO_2 at the finer scale with corresponding observations at 969 national air quality monitoring sites. The modeled meteorological variables, including temperatures at 2 m, wind speeds and directions at 10 m, were also validated with the 3-hour observational data set at 136 sites obtained from the National Centers for Environmental Information (https://www.ncei.noaa.gov/, last access: March 2025). Seven statistical metrics were used to determine the performance of the model. The metrics include normalized mean bias (NMB), mean normalized bias (MNB), mean fractional bias (MFB), mean normalized absolute error (MNAE), mean absolute error (MAE), root mean square error (RMSE), and Pearson correlation coefficient (R) (Brasseur and Jacob, 2017). Table S7 provides information on their functions.

https://doi.org/10.5194/egusphere-2025-268
Preprint. Discussion started: 26 March 2025

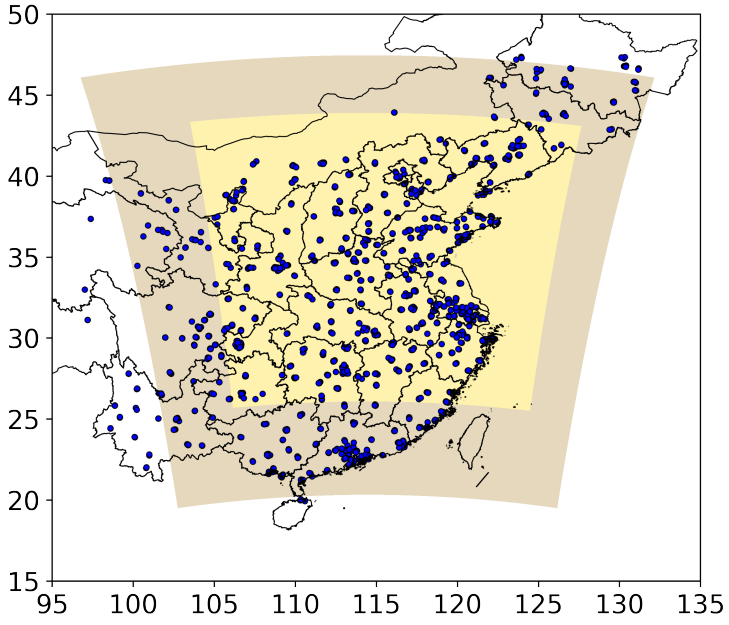

Figure 2. Model domains employed for WRF-Chem simulations in eastern China. The horizontal resolution of the outer Domain 01 (depicted in gray) is 36 km, featuring 75×86 grids, including a total of observed 1372 sites (in dark blue). The inner Domain 02 (illustrated in yellow) has a higher horizontal resolution of 12 km, with 160×166 grids, covering observed 969 sites (in dark blue).

https://doi.org/10.5194/egusphere-2025-268
Preprint. Discussion started: 26 March 2025

3 Results and discussion

3.1 Sectoral emissions and comparison

CINEI shows the comprehensive sectoral anthropogenic emissions and reveals significant changes in ozone precursor emissions (NO_x, CO and NMVOCs) in China (Fig. 3a-c). These include the decrease in NO_x emissions (-0.9±2.9 Tg yr^{-1}) since 2012 and CO emissions (-7.0±23.4 Tg yr^{-1}) since 2008 and the increase of NMVOC emissions (0.4±1.0 Tg yr^{-1}) from 2008 to 2019. CINEI also showed a slight decrease in 2020 due to the COVID-19 shutdown (Zheng et al., 2021a). In general, the major sectors in the global inventories show a greater divergence from the national inventories. There is a of approximately 5% for NO_x of power generation with respect to the total emissions of CINEI, and a deviation of more than 10% for HTAP and CAMS CO from residential activities. The deviations in the totals are minimal and the sectors are more comprehensive by including the main sectors from the national inventory and key sectors (ships, waste, etc., as discussed in Text S6 and Tables S11-S13).). Global inventories (HTAP and CEDS) agree well with the national (MEIC) in terms of total emission levels and multi-year changes in China (Fig. 3g-i). However, emissions in CAMS show notable differences from those in other inventories: CAMS estimates lower NO_x and CO emissions in China before 2014; CAMS displays the variation without rapid reduction during the study period (Fig. 3d-f).

CINEI also provides the amount of emissions from eight anthropogenic sectors (Fig. 3a-c). The main sectors of the CINEI in China include industry (NO_x, CO, NMVOCs), transportation (NO_x, CO, NMVOCs), energy (NO_x, CO, NMVOCs), and transport (NO_x, CO, NMVOCs), power (NO_x) and residential (CO, NMVOCs). Compared to MEIC, CINEI includes the contributions of the marine sector to NO_x emissions, the waste sector to CO emissions, and the agricultural sector to NMVOC emissions (Fig. 3d-f). Ignoring these emissions can lead to bias in the estimation of anthropogenic emissions and in the simulation of ozone (von Schneidemesser et al., 2023). Differences in sectoral emissions (CINEI minus other inventories) are evident in major and omitted sectors (Fig. 3d-f). In general, emissions from the power sector are often higher in the three global inventories, while those from the transport sector are mostly lower. The apparently lower NO_x from transport and CO from residential emissions in CAMS (and EDGAR) are mainly due to underestimated contributions. Although CEDS provides total emission estimates closer to those of CINEI for China, there are still notable differences in the contributions of certain sectors. In particular, the energy and residential sectors contribute more to NO_x emissions, but lower emissions from shipping and industry offset these increases. Higher NMVOC emissions from the power sector are offset by those from the industry sector. This is similar to the comparison of sectoral emissions in HTAP and CINEI.

We also analyzed the contributions of sectoral emissions to changes in total emissions and identified the key sectors for emission changes of each pollutant. Table S14 summarizes the linear trends (slopes) of 8 sectoral emissions for NO_x, CO, and NMVOCs from 2008 to 2020, and the piece-wise slopes for sectoral emissions that show changes with increases followed by decreases (Table S15). The power sector is the key sector driving the decrease in NO_x emissions, while most of the other sectors lead to increasing NO_x emissions. The changes in the power sector correspond well with the rapid decrease in NO_x emissions from power generation in MEIC v1.4 (Fig. S8), indicating the effect of the introduction of cleaner energy in power plants (Yan et al., 2023). The major sectors contributing to the reduction in CO emissions over the study period include industry (60%

https://doi.org/10.5194/egusphere-2025-268
Preprint. Discussion started: 26 March 2025

reduction), residential (29%), and transportation (16%). Emissions from more specific sources, including the petrochemical industry, cooking, and gasoline-powered vehicles, also show significant reductions in MEIC v1.4 (Fig. S9). In addition, industry is driving the increase in NMVOC emissions, despite the decrease in NMVOC emissions from the residential and transportation sectors. These NMVOC emissions are associated with industrial painting, iron and steel industry, and architectural coatings in MEIC v1.4 (Fig. S10). Thus, more efforts are warranted in the future to control NMVOC emissions from industrial processes in China.

In addition, ozone precursor emissions from the four missing sectors in the MEIC (ships, waste, agriculture and aviation) are all increasing. NO_x emissions of HTAP from shipping show an increasing trend of 0.10 ± 0.01 Tg yr^{-1}. This trend appears to offset the decrease in NO_x emissions from the energy sector. We have therefore identified shipping, waste, aviation and agriculture as key sectors due to their inverse relationship with total emission changes (Tables S11-S13). Therefore, ignoring sectoral emissions of ozone precursors may lead to biased attribution results of ozone changes.

https://doi.org/10.5194/egusphere-2025-268
Preprint. Discussion started: 26 March 2025

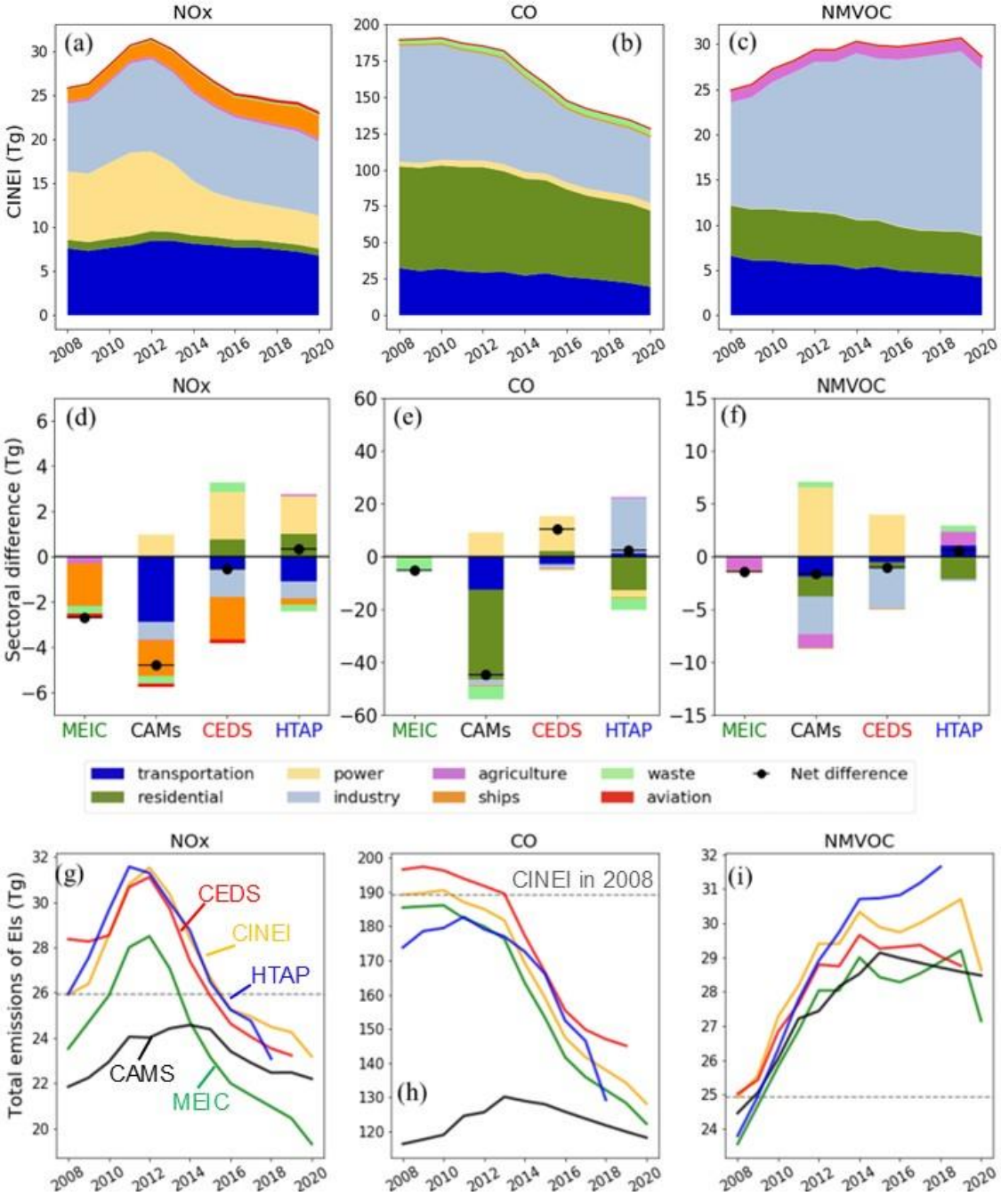

Figure 3. The top panels (a-c) show the interannual variability of NO_x (NO_2), CO, and NMVOC emissions across eight aggregated sectors in the CINEI, and all data are listed in Tables S8-S10. The middle panels (d-f) depict the averaged annual differences from 2008 to 2018 in sectoral emissions between each of the four inventories and CINEI (existing inventories minus CINEI). Sectoral emissions are indicated by bars and total emissions by dots. The findings are based on the mean differences from 2008 to 2018, and the results for each year are shown in Fig. S11. The bottom panels (d-f) present the interannual variability of total NO_x (NO_2), CO and NMVOC emissions in China from the CINEI (in orange) and four selected emission inventories (MEIC in green, CAMS in black, CEDS in red, and HTAP in blue). Total emissions from 8 sectors used from multiple inventories are provided in Tables S12-S14.

https://doi.org/10.5194/egusphere-2025-268
Preprint. Discussion started: 26 March 2025

3.2 Speciation of NMVOCs emission

The increase in NMVOC emissions is a potential contributor to severe ozone pollution in China (Li et al., 2019; Zhang et al., 2021). Individual NMVOC species often differ in the amounts emitted and in their ozone formation potential, and thus contribute differently to ozone formation. We ranked the top 20 NMVOC species in China according to their mean annual emissions in CINEI and quantified their OFPs values (Fig. 4a). These NMVOCs species cumulatively contribute to more than 85% of the total OFPs by NMVOCs emissions, indicating their notable influence on ozone pollution. In general, NMVOCs species with more abundant emissions tend to contribute more to OFPs, such as m/p-xylene and toluene, which together have an OFP value of 23.1 Tg-O_3 on an annual average from 2008 to 2020 (23.4% of the total OFPs). Propene, o-xylene and ethene, with higher OH reactivity (characterized by their MIR values), also have significant contributions to total OFPs (propene 13.9 Tg-O_3 and 14.1% in percentage contribution to total OFP, o-xylene 7.1 Tg-O_3 and 7.2%, and ethene 6.9 Tg-O_3 and 6.1%). In contrast, high emissions of ethylbenzene and styrene (10% of total NMVOC emissions) contribute only 7.2 Tg-O_3 (6%) to the total OFPs due to their low reactivity. Regarding the OFPs of different NMVOC groups, aromatics and alkenes contribute to 75% of the total OFPs as shown in Fig. S12. This result is in good agreement with previously reported results (Li et al., 2019; Wu et al., 2022). The OFPs values in VOCs categories are also compared with the result of previous studies (Table S16). The emission and OFPs of all NMVOCs species on annual averages also for mainland China are shown in Tables S19 and S20.

Targeting the emission sectors most associated with NMVOC species with high OFP values may be efficient for ozone abatement. The sectoral contributions to the top 20 NMVOC species are shown in Figure 4b. M/p-xylene, toluene, propene and o-xylene emissions are mainly from industrial sources (70%). This includes their use as solvents in industrial processes (e.g. industrial painting and architectural coatings). The residential sector is also an important contributor to these NMVOC species, accounting for 20-30%. Ethylene emissions show different characteristics: besides the significant contributions from the industrial and residential sectors, agriculture also accounts for a large share (32%), as does transport (25%), indicating the contributions from fishing, harvesting and diesel vehicles. For the other NMVOC species in the top 20, industry and transport are mostly the main sources and therefore NMVOC emission control should focus on the contributions of these two sectors. For formaldehyde and acetaldehyde emissions, the agricultural sector is the main source, together with emissions from crop burning (including burning of rice and wheat straw, maize, etc.). Ignoring agricultural NMVOC emissions in anthropogenic emission inventories may lead to an underestimation of the contribution of these species to ozone pollution. Finally, for the three remaining sectors missing from the MEIC (waste, ships, and aviation), their overall contributions to emissions of the top 20 NMVOC species are limited (McDonald et al., 2018).

Targeting the emission sectors most related to NMVOC species with high OFP values may be efficient for ozone mitigation. The sectoral contributions to the top 20 NMVOC species are shown in Fig. 4b. M/p-xylene, toluene, propene and o-xylene emissions are mainly derived from the industrial sources (~70%). This involves their usage as solvents in industrial processes (e.g., industrial painting and architectural coatings). The residential sector also has an important contribution to these NMVOC species, accounting for 20-30%. Ethene emissions show different characteristics: besides the considerable contributions of the industrial and residential sectors, agriculture also accounts for a large proportion (32%) as does transportation (25%), indicating

https://doi.org/10.5194/egusphere-2025-268
Preprint. Discussion started: 26 March 2025

the contributions of fishing and harvesting and diesel vehichles. For the other NMVOC species among the top 20, industry and transportation are mostly the major sources, and therefore NMVOC emission control should focus on the contributions of these two sectors. For formaldehyde and acetaldehyde emissions, the agricultural sector is the main source, related to the emissions along with crop burning (including the burning of rice and wheat straw, maize, etc.). Ignoring agricultural NMVOC emissions in anthropogenic emission inventories can lead to underestimated contributions of these species to ozone pollution. Finally, for the three remaining sectors that are missing in MEIC (waste, ships and aviation), their contributions to the emissions of the top 20 NMVOC species are overall limited (McDonald et al., 2018).

To evaluate the NMVOC speciation used in CINEI, we selected 9 hydrocarbon species and used their emission ratios to C_2H_2 (mol/mol) for comparison with those in global and national inventories, as well as with observations over China (Figure S13). We used C_2H_2 instead of CO because C_2H_2 and hydrocarbons are monitored with the same measurement system (GC MS/FID). The in situ measurements of VOC species (in ppbv) were obtained from the literature (Lv et al., 2021; Huang et al., 2022; Li et al., 2022; Song et al., 2021). These data, obtained from megacities (Beijing, Shanghai, etc.) and provincial capitals, are listed in Tables S17-S18. We extracted emissions at the same locations and dates and calculated the ratios of hydrocarbons to C_2H_2. The selected VOCs have similar atmospheric lifetimes and sources in urban areas, primarily from transportation and industrial emissions. Species treated as a single entity in emission inventories (e.g., ketones) and those not comparable to observations (e.g., oxygenated VOCs) were excluded from the analysis. Our comparison showed that NMVOC speciation from emission inventories is quite uncertain due to the applied source profiles, different sectoral distributions and emission masses. The ratios in the CINEI are closer to the observations, except for ethene and xylene. In contrast, the global and MEIC inventories have lower ratios for alkanes compared to observations, possibly due to misrepresentation of the dominant sectoral emission (solvent or industry) for these species. However, the ratios of primary alkenes (ethene and propene) in the MEIC and CINEI exceed the observed values. Alkenes have faster loss rates via OH, which may lead to alkenes from primary source are degraded immediately. Therefore, the observed ratios of alkenes to C_2H_2 may be lower than its emission ratios (MIR > 9). Therefore, the speciation of NMVOC emissions. Improving this description would also influence the homogenization of the national inventory with global ones and the application of CTM simulations.

https://doi.org/10.5194/egusphere-2025-268
Preprint. Discussion started: 26 March 2025

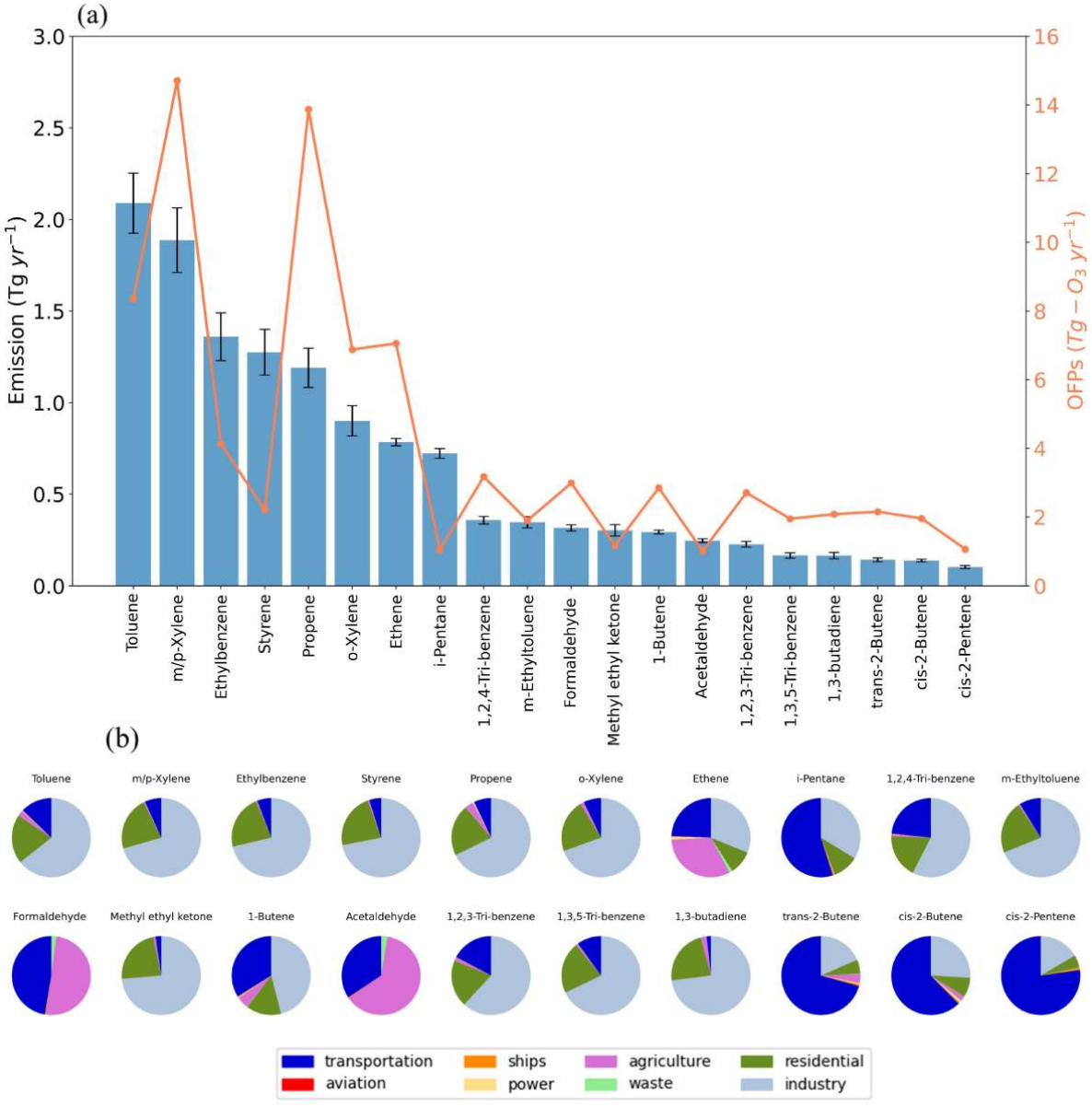

Figure 4. (a) Mean annual emissions (blue bars in Tg yr^{-1}) and OFPs (yellow line in Tg-O_3 yr^{-1}) of the top 20 NMVOCs species in CINEI (ranked by emission amount). Error bars at the top of the columns represent the standard deviations of the emissions from 2008 to 2020. (b) Sectoral contributions to the emissions of the top 20 NMVOC species. Emissions and OPFs of all NMVOC species in 8 sectors are provided in Table S19 and Table S20 respectively.

https://doi.org/10.5194/egusphere-2025-268
Preprint. Discussion started: 26 March 2025

3.3 Harmonizing emissions on spatial scales

Fig. 5 shows the spatial distribution of NO_x emissions from the CINEI dataset across eight sectors in East Asia in 2017. For emissions outside of China, we use CEDS emissions for the major sectors because CEDS incorporates national emissions from surrounding countries and is widely used in global CTM models (Hoesly et al., 2018). We chose NO_x as a representative species to analyze the spatial distribution of pollutant emissions in CINEI. Emission maps for other species(SO_2, NH_3, CO, C_2H_6, toluene, and C_2H_4) from CINEI are shown in Fig. S15.

Anthropogenic emissions, such as those from the residential, transportation, and waste sectors, tend to be high in densely populated areas of northern and eastern China, Japan, Korea, and India, indicating their close association with human activities (see Fig. S14 for population distribution). NO_x emissions from the energy and industry sectors, which are considered point sources, are characterized by hotspots at sites for electricity generation, solvent volatilization, and cement, iron, and steel production. The convergence of these sectoral data from the national emission inventory and CEDS for surrounding countries in CINEI is tested by Monte Carlo simulations with comparisons to CEDS data. The Monte Carlo uncertainties of the two datasets are of the same order of magnitude, indicating that the possibility density of the CINEI is normal on the spatial distribution and not separated into two datasets.

The distribution of shipping reveals shipping routes in the ocean and inland rivers. Aviation emissions distribution is related to airline connections between different airports, with high values likely occurring near major airports in China. The emissions of other pollutants suggest similar characteristics of spatial distributions (Figure S15).

In addition, harmonized emission inventories used the default emissions for total emission amount from the national inventory, but emissions outside China were taken from the three global inventories. To illustrate the difference in emissions in mainland China and the similarity in emissions outside of China between national and global inventories, the distributions of the paired comparisons (HM_CEDS vs. CEDS, HM_CAMS vs. CAMS, HM_HTAP vs. HTAP) are also shown in Figs. S16-S19.

https://doi.org/10.5194/egusphere-2025-268
Preprint. Discussion started: 26 March 2025

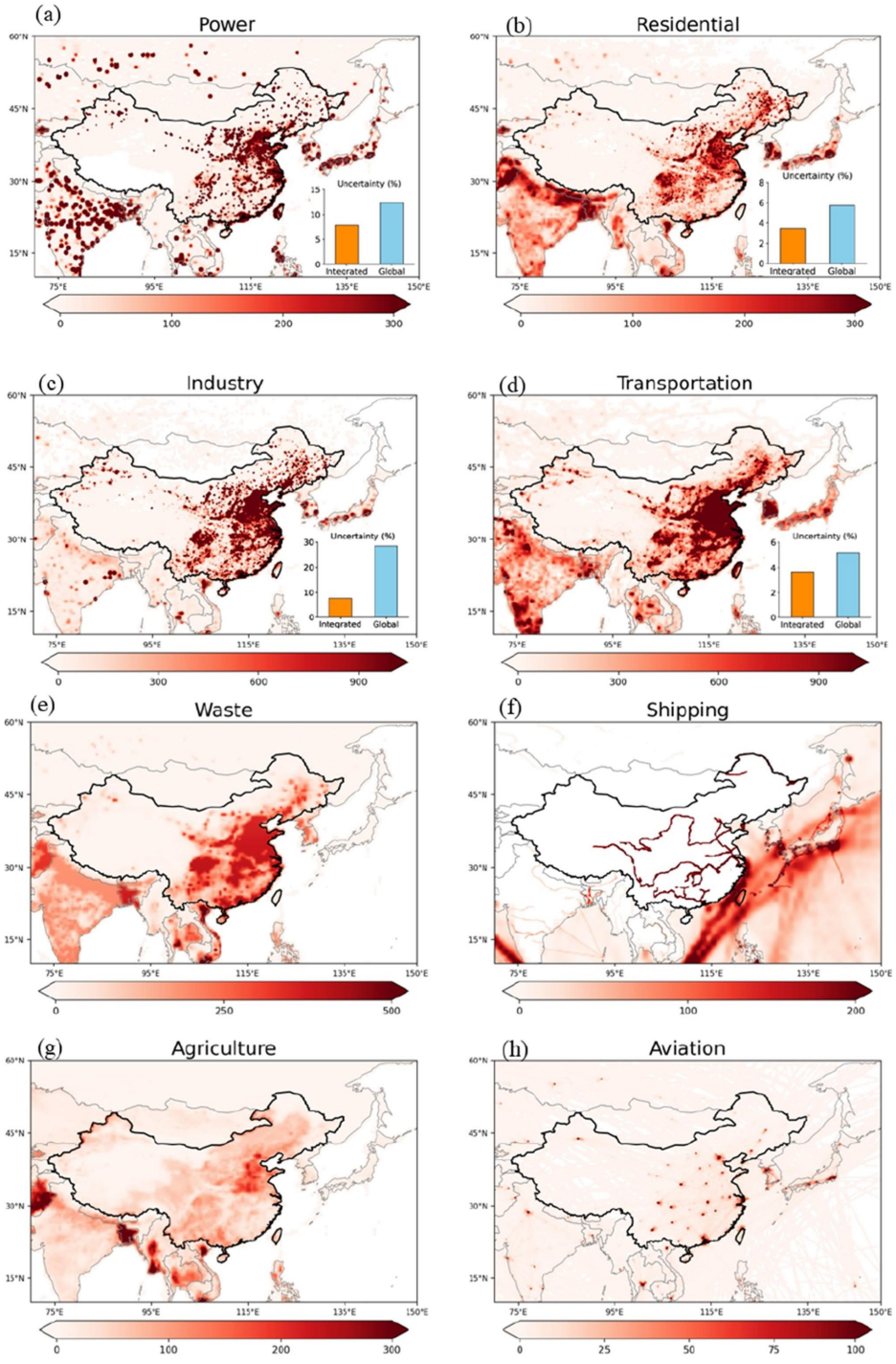

Figure 5. Spatial distribution of NO_x (NO_2) emissions (unit: ton $grid^{-1}$ yr^{-1}) from eight sectors in East Asia in 2017, and for power, residential, industry, transport sectors, we add comparisons of Monte Carlo uncertainties between integrated (CINEI in orange) and global inventory (CEDS, in blue).

https://doi.org/10.5194/egusphere-2025-268
Preprint. Discussion started: 26 March 2025

3.4 Comparisons of simulation results based on multiple anthropogenic emission inventories

To identify the most harmonized inventories suitable for regional simulations over China, the performance of WRF-Chem modeling results based on the national inventory (MEIC) merged into three global inventories (HM_CEDS, HM_CAMS, and HM_HTAP) has been were evaluated. The three harmonized inventories show minimal variation in the averages over the entire domain where the grid contains observed sites (Text S10). The normalized mean biases (NMBs) among the three modeling results are 10% and 40% for ozone in summer and winter, respectively, -0.5% in summer and 40% in winter for NO_2 and -50% for CO for both seasons (Fig. S20). However, HM_CEDS shows better agreement with observations from coastal cities, which have a deeper response to the transport of emissions to mainland China. In contrast, HM_CAMS and HM_HTAP have significant biases. Accordingly, HM_CEDS was selected to represent all harmonized inventories for subsequent modeling comparisons, hereafter abbreviated as HMEI.

To further evaluate the performance of CINEI, HMEI and global inventories (CAMS, CEDS, HTAP), anthropogenic emissions (NO_x, CO and NMVOCs) are shown in the upper panels of Fig. 6 and 7, and modeling results (O_3, NO_2 and CO mixing ratios) are compared with observations in the lower panels of Fig. 6 and 7. In both months the O_3 mixing ratios are overestimated by CINEI (12% in summer and 42% in winter) and HMEI (20% and 40% NMB). The NO_2 mixing ratios of CINEI are closer to the observations by about 5% in summer and 40% in winter. The differences found between the two emission inventories can be attributed to the aggregation of shipping, waste and aviation emissions in the CINEI dataset. These sectors lead to a small increase in emissions (less than 10%) in the CINEI inventory. Additional statistical analysis shows that CINEI and HMEI have superior performance compared to global inventories (Text S11 and Fig. S23-24). The MFB for CINEI is ± 0.3 in both seasons and the MNAE is less than 0.5, within the ranges suggested in the literature (Zhai et al., 2024). However, the CO mixing ratios are apparently underestimated in all cases (up to 50% NMB). The underestimation of CO likely has links with (1) differences between urban and regional CO backgrounds, as (Zhao et al., 2012) reported using satellite data; (2) the inaccurate OH mixing ratios in CTM leading to more CO sink (Gaubert et al., 2020). Therefore, both both CINEI and HMEI result in reliable model performance.

Among the three global inventories, the CEDS result is in better agreement and slightly closer to the observations, with O_3 NMB 6% and NO_2 NMB -24% in summer (47% and 5% in winter). In the two seasons, the NO_x emissions of CEDS are about -18% lower than that of CINEI, but the NMVOC emissions are about -50% lower than that of CINEI. In addition, CAMS underestimates anthropogenic emissions of all precursors in both summer and winter. In particular, in July 2017, NMVOC emissions are 90% lower in CAMS than in CINEI. As a consequence, O_3 mixing ratios in summer (winter) are underpredicted by -31% NMB (-26%) (for more details, see Supplementary Text S11 and accompanying figures). An unexpected result is that the NO_2 mixing ratios are overpredicted by ~35% in CAMS, despite the lower NO_x emissions in CAMS. In contrast, HTAP has the highest emissions for the two studied months in all inventories, and the HTAP NO_2 mixing ratio is the highest in both seasons with 113% NMB (summer) and 121% (winter). Detailed statistical indices for these comparisons are provided in Supplementary S11 and accompanying figures. However, the HTAP O_3 mixing ratio is overpredicted in summer and largely underpredicted in winter. The comparisons and validations suggest that ozone changes are non linearly related to anthropogenic

https://doi.org/10.5194/egusphere-2025-268
Preprint. Discussion started: 26 March 2025

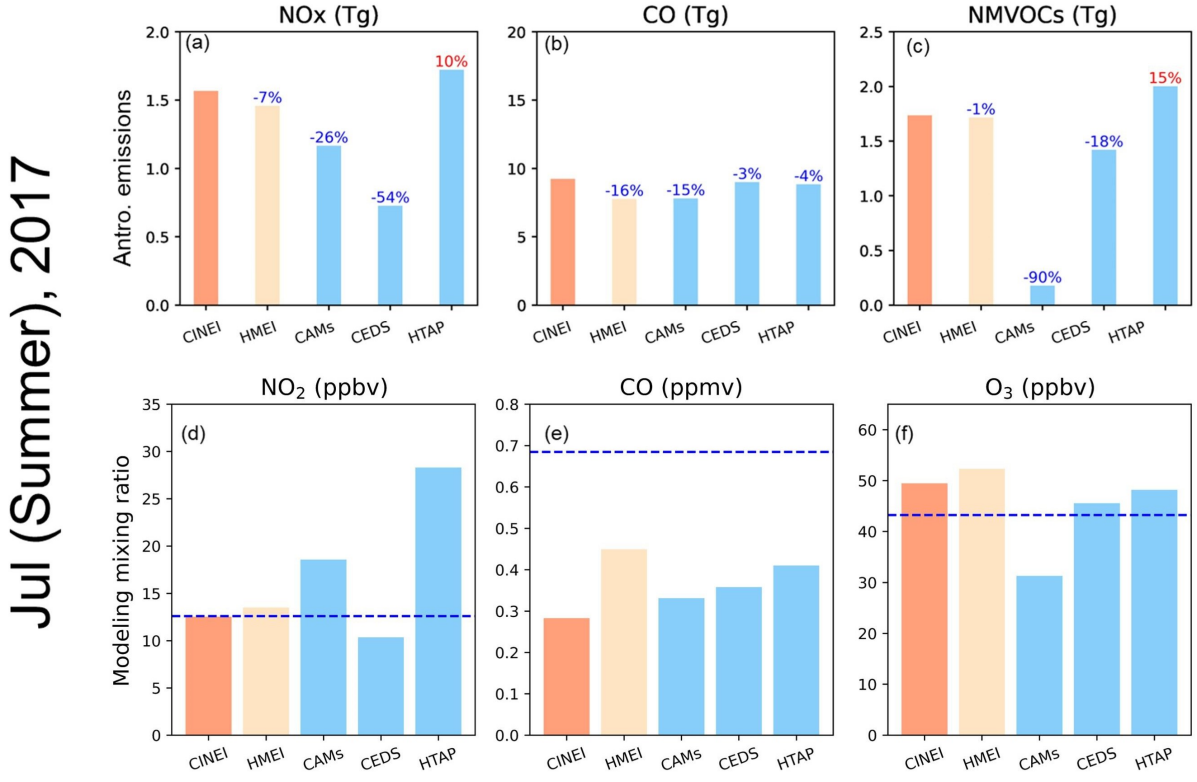

Figure 6. The top panels (a-c) present total anthropogenic emission differences of ozone precursors (NO_x, CO, and NMVOC) for July 2017 between the CINEI, HMEI, CAMS, CEDS, and HTAP inventories using the CINEI integrated emission inventory as a reference. Bottom panels (d-f) show WRF-Chem simulated mixing ratios of O_3, NO_2, and CO for the same month and within the modeling domain (latitudes from 25.5° to 43.6°; longitudes from 103.5° to 127.6°) using the different emission inventories. Individual columns show simulated mean mixing ratios in the model domain for each emission inventory used. The dashed blue lines show average observed mixing ratios calculated using the stations within the specified domain.

emissions of ozone precursors. Emissions and concentrations of precursors of O_3 may also alter total OH loss rates (L_{OH}) and further affect radical termination processes and ozone production rates.

https://doi.org/10.5194/egusphere-2025-268
Preprint. Discussion started: 26 March 2025

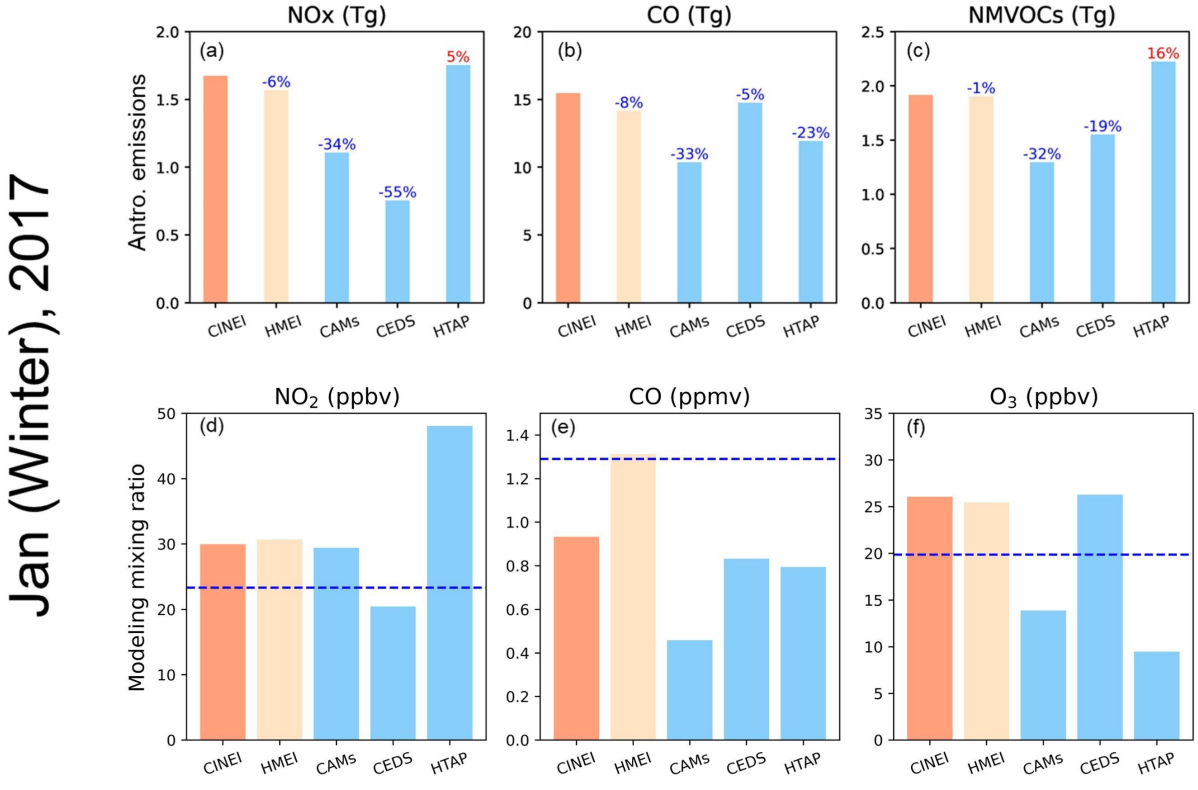

Figure 7. Same content with Figure 6, but in January 2017.

https://doi.org/10.5194/egusphere-2025-268
Preprint. Discussion started: 26 March 2025

4 Conclusions

The development of anthropogenic emission inventories used in simulations by CTMs faces various challenges, such as accurate descriptions of emissions from complete sectors and with complete spatial coverage, as well as rapid emission changes due to regional mitigation. In this study, we developed two new types of anthropogenic emission inventories for China to better meet the requirements in the study of long-term ozone changes:

- The harmonized inventories, HMEIs, combine emissions in mainland China from MEIC and emissions in regions outside China from three different global emission inventories (CAMS, CEDS, HTAP).
- The integrated inventory, CINEI, is based on the harmonized inventory (harmonized MEIC with CEDS), but additionally includes from the global inventories the emissions in China contributed by the missing emission sectors in the MEIC, including ships, waste, aviation, and agriculture.

To perform the integration, the emission sector types, spatial resolutions, and NMVOC speciation were made consistent between the MEIC and the global emission inventories. The emission processing system developed for this study (Fig. 1a) is able to meet these requirements. To evaluate the performance of harmonized and integrated inventories in the simulation of ground-level ozone, we generated emission inventories for East Asia in two representative months (January and July 2017), applied them in the simulations of WRF-Chem, and compared the model results with the corresponding observations. The results show that the application of harmonized and integrated inventories leads to a satisfactory performance in the simulation of ozone and two of its precursors, NO_2 and CO. In contrast, the direct application of global emission inventories (HTAP and CAMS) can lead to a significant bias in the simulation results. The construction of our integrated emission inventories provides valuable insights for designing ozone mitigation strategies and refining anthropogenic inventories for China:

1. CINEI and HMEI show acceptable model performance when evaluated against observations and compared with simulations driven by global inventories. In summer, the CINEI model results overestimate the mixing ratios of ozone by 5% and those of NO_2 by 0.5%. In winter, ozone is overestimated by 5.8 ppb, or 40%. CO is underestimated by about 30-50% in both seasons, which is common to all simulation cases. However, the model performance needs to be further improved and further studies are needed to reduce the bias by implementing better meteorological fields, chemical mechanisms, parameterizations of dynamical processes and deposition based on comprehensive comparisons with observations from different sources.

2. The CEDS is a good option for providing emission data outside mainland China because of its better modeling performance (O_3 and NO_2 NMB < 10%) compared to CAMS and HTAP. Due to its moderately long lifetime, ozone can be transported from regions outside China (Zheng et al., 2021b; Qu et al., 2024). We found that the modeled ozone mixing ratios for three harmonized inventories differ from observations by 2 to 6 ppbv on spatial average. Thus, the selection of inventories for the surrounding regions of China is also imperative for ozone simulations in China. The applicability of the MOSAIC emission inventory product needs to be validated based on comparisons between observations and CTM results driven by MOSAIC emissions.

https://doi.org/10.5194/egusphere-2025-268
Preprint. Discussion started: 26 March 2025

3. Ozone precursor emissions from sectors initially omitted from the national inventory may be significant, such as NO_x emissions from ships (~1 Tg yr^{-1}) and CO emissions from waste (~5 Tg yr^{-1}). The omission of these emissions may lead to inconsistencies in the results of ozone simulations and overlook their potential role in ozone control.

4. Additional measures are needed to curb the increase in NMVOC emissions, despite effective reductions in NO_x (-0.9 Tg yr^{-1}) and CO emissions (-7 Tg yr^{-1}) over the past 10 years. In particular, the reduction of key species and sources of NMVOC emissions, such as m/p-xylene and toluene from solvents and ethene from diesel vehicles, will be effective in reducing ozone in China due to the larger OFP of these species. Further research is needed to support the formulation of effective strategies for future ozone control in China.

In a follow-up study, we will investigate the ability of CINEI, with updated speciated NMVOC emissions and more sectoral emissions, to better represent total OH loss rates and contributions to ozone formation rates. As ozone mixing ratios do not respond linearly to changes in ozone precursor emissions, the geographical extent of VOC and NO_x restricted areas appears to change with the emission inventories adopted. We discuss the ozone photochemistry regime under different emission scenarios and propose more insightful and strategic emission scenarios.

https://doi.org/10.5194/egusphere-2025-268
Preprint. Discussion started: 26 March 2025

Code availability. The python tool to create the integrated emission data (CINEI) is archived in Zenodo website (https://doi.org/10.5281/zenodo.15000795) (Zhang, 2025a). WRF-Chem model code can be found in the GitHub (https://github.com/wrf-model/WRF/releases, last accessed: March 2025) (Skamarock et al., 2019).

Data availability. Integrated emission (CINEI) data are archived in PANGAEA website (https://doi.pangaea.de/10.1594/PANGAEA.974347)(Zhang et al., 2025). HTAP emission data can be accessed from the Zenodo website (https://doi.org/10.5281/zenodo.7516361) (Monica, 2023). CEDS emission data are available from the Zenodo website (https://doi.org/10.5281/zenodo.12803197) (Hoesly et al., 2024). National (MEIC) and CAMs emission data are available at their official websites (http://meicmodel.org.cn/?page_id=1772&lang=en and https://eccad.sedoo.fr/, respectively, last accessed: March 2025) (Zheng et al., 2018; Soulie et al., 2023). Due to occasional maintenance of the MEIC and CAMS websites, we have uploaded the data used in this study to Zenodo (https://doi.org/10.5281/zenodo.15039737) (Zhang, 2025b).

Author contributions. YZ, GB, MK and MV developed the concept of the manuscript. YZ performed the formal analysis of the data, performed the experiments. YZ drafted the manuscript. CG provided emission data. NK, AP, and KQ provided technical support; all coauthors revised and edited the manuscript.

Competing interests. The contact author has declared that none of the authors has any competing interests.

Acknowledgements. Work performed within the Air-Changes (Air pollution in China and the undesired effects of mitigation strategies) Sino-German DFG project. The simulations were performed on the HPC cluster Aether at the University of Bremen, financed by DFG within the scope of the Excellence Initiative.

YZ is supported by China Scholarship Council (CSC) for PHD study (NO.202006040059). This research has been supported by the Deutsche Forschungsgemeinschaft (Air-Changes, grant no. 4487-20203) and the National Natural Science Foundation of China (grant no. 42293322).

https://doi.org/10.5194/egusphere-2025-268
Preprint. Discussion started: 26 March 2025

References

12th Five-Year Plan: The Outline of the National 12th Five-Year Plan on Economic and Social Development, https://www.gov.cn/2011lh/content_1825838_2.htm, accessed: March 2025, 2011.

Brasseur, G. P. and Jacob, D. J.: Modeling of Atmospheric Chemistry, https://api.semanticscholar.org/CorpusID:98910532, 2017.

Carter, W. P.: Development of ozone reactivity scales for volatile organic compounds, Journal of the Air and Waste Management Association, 44, 881–899, https://doi.org/10.1080/1073161x.1994.10467290, 1994.

Carter, W. P.: Development of a database for chemical mechanism assignments for volatile organic emissions, https://doi.org/10.1080/10962247.2015.1013646, 2015.

Chang, X., Zhao, B., Zheng, H., Wang, S., Cai, S., Guo, F., Gui, P., Huang, G., Wu, D., Han, L., et al.: Full-volatility emission framework corrects missing and underestimated secondary organic aerosol sources, One Earth, 5, 403–412, https://doi.org/10.1016/j.oneear.2022.03.015, 2022.

Crippa, M., Guizzardi, D., Pisoni, E., Solazzo, E., Guion, A., Muntean, M., Florczyk, A., Schiavina, M., Melchiorri, M., and Hutfilter, A. F.: Global anthropogenic emissions in urban areas: patterns, trends, and challenges, Environmental Research Letters, 16, 074 033, https://doi.org/10.1088/1748-9326/ac00e2, 2021.

Crippa, M., Guizzardi, D., Butler, T., Keating, T., Wu, R., Kaminski, J., Kuenen, J., Kurokawa, J., Chatani, S., Morikawa, T., Pouliot, G., Racine, J., Moran, M. D., Klimont, Z., Manseau, P. M., Mashayekhi, R., Henderson, B. H., Smith, S. J., Suchyta, H., Muntean, M., Solazzo, E., Banja, M., Schaaf, E., Pagani, F., Woo, J.-H., Kim, J., Monforti-Ferrario, F., Pisoni, E., Zhang, J., Niemi, D., Sassi, M., Ansari, T., and Foley, K.: The HTAP_v3 emission mosaic: merging regional and global monthly emissions (2000–2018) to support air quality modelling and policies, Earth System Science Data, 15, 2667–2694, https://doi.org/10.5194/essd-15-2667-2023, 2023.

Doumbia, T., Granier, C., Elguindi, N., Bouarar, I., Darras, S., Brasseur, G., Gaubert, B., Liu, Y., Shi, X., Stavrakou, T., Tilmes, S., Lacey, F., Deroubaix, A., and Wang, T.: Changes in global air pollutant emissions during the COVID-19 pandemic: A dataset for atmospheric modeling, https://doi.org/10.5194/essd-13-4191-2021, 2021.

Dukowicz, J. K.: Conservative rezoning (remapping) for general quadrilateral meshes, Journal of Computational Physics, 54, 411–424, https://doi.org/10.1016/0021-9991(84)90125-6, 1984.

Emmons, L. K., Schwantes, R. H., Orlando, J. J., Tyndall, G., Kinnison, D., Lamarque, J.-F., Marsh, D., Mills, M. J., Tilmes, S., Bardeen, C., et al.: The chemistry mechanism in the community earth system model version 2 (CESM2), Journal of Advances in Modeling Earth Systems, 12, https://doi.org/10.1029/2019MS001882, 2020.

Feng, L., Smith, S. J., Braun, C., Crippa, M., Gidden, M. J., Hoesly, R., Klimont, Z., Van Marle, M., Van Den Berg, M., and Van Der Werf, G. R.: The generation of gridded emissions data for CMIP6, https://doi.org/10.5194/gmd-13-461-2020, 2020.

Gaubert, B., Emmons, L. K., Raeder, K., Tilmes, S., Miyazaki, K., Arellano Jr., A. F., Elguindi, N., Granier, C., Tang, W., Barré, J., Worden, H. M., Buchholz, R. R., Edwards, D. P., Franke, P., Anderson, J. L., Saunois, M., Schroeder, J., Woo, J.-H., Simpson, I. J., Blake, D. R., Meinardi, S., Wennberg, P. O., Crounse, J., Teng, A., Kim, M., Dickerson, R. R., He, H., Ren, X., Pusede, S. E., and Diskin, G. S.: Correcting model biases of CO in East Asia: impact on oxidant distributions during KORUS-AQ, Atmospheric Chemistry and Physics, 20, 14 617–14 647, https://doi.org/10.5194/acp-20-14617-2020, 2020.

Gery, M. W., Whitten, G. Z., Killus, J. P., and Dodge, M. C.: A photochemical kinetics mechanism for urban and regional scale computer modeling, Journal of Geophysical Research: Atmospheres, 94, 12 925–12 956, https://doi.org/10.1029/JD094iD10p12925, 1989.

https://doi.org/10.5194/egusphere-2025-268
Preprint. Discussion started: 26 March 2025

Granier, C., Darras, S., Denier Van Der Gon, H., Jana, D., Elguindi, N., Bo, G., Michael, G., Marc, G., Jalkanen, J.-P., and Kuenen, J.: The Copernicus Atmosphere Monitoring Service global and regional emissions (April 2019 version), pp. 1–55, https://hal.archives-ouvertes.fr/hal-02322431, 2019.

Guenther, A. B., Jiang, X., Heald, C. L., Sakulyanontvittaya, T., Duhl, T., Emmons, L. K., and Wang, X.: The Model of Emissions of Gases and Aerosols from Nature version 2.1 (MEGAN2.1): an extended and updated framework for modeling biogenic emissions, Geoscientific Model Development, 5, 1471–1492, https://doi.org/10.5194/gmd-5-1471-2012, 2012.

Heuvelink, G. B. and Brus, D. J.: Monte Carlo and spatial sampling effects in regional uncertainty propagation analyses, https://core.ac.uk/reader/29249090, 2009.

Hodzic, A. and Knote, C.: MOZART gas-phase chemistry with MOSAIC aerosols, NCAR/ACD. Readme Document, 449, https://www2.acom.ucar.edu/sites/default/files/documents/MOZART_MOSAIC_V3.6.readme_dec2016.pdf, 2014.

Hoesly, R., Smith, S. J., Prime, N., Ahsan, H., Suchyta, H., O'Rourke, P., Crippa, M., Klimont, Z., Guizzardi, D., Behrendt, J., Feng, L., Harkins, C., McDonald, B. C., Mott, A., McDuffie, E. E., Wang, S., and Nicholson, M. B.: CEDS v_2024_10_21 Release Gridded Emissions Data 0.5 degree (v_2024_10_21) [Data set], https://doi.org/10.5281/zenodo.13952845, 2024.

Hoesly, R. M., Smith, S. J., Feng, L., Klimont, Z., Janssens-Maenhout, G., Pitkanen, T., Seibert, J. J., Vu, L., Andres, R. J., Bolt, R. M., Bond, T. C., Dawidowski, L., Kholod, N., Kurokawa, J. I., Li, M., Liu, W., Lu, Z., Moura, M. C., O'Rourke, P. R., and Zhang, Q.: Historical (1750-2014) anthropogenic emissions of reactive gases and aerosols from the Community Emissions Data System (CEDS), https://doi.org/10.5194/gmd-11-369-2018, 2018.

Huang, A., Yin, S., Yuan, M., Xu, Y., Yu, S., Zhang, D., Lu, X., and Zhang, R.: Characteristics, source analysis and chemical reactivity of ambient VOCs in a heavily polluted city of central China, Atmospheric Pollution Research, 13, 101 390, https://doi.org/10.1016/j.apr.2022.101390, 2022.

Huang, G., Brook, R., Crippa, M., Janssens-Maenhout, G., Schieberle, C., Dore, C., Guizzardi, D., Muntean, M., Schaaf, E., and Friedrich, R.: Speciation of anthropogenic emissions of non-methane volatile organic compounds: a global gridded data set for 1970–2012, Atmospheric Chemistry and Physics, 17, 7683–7701, https://doi.org/10.5194/acp-17-7683-2017, 2017.

Iacono, M. J., Delamere, J. S., Mlawer, E. J., Shephard, M. W., Clough, S. A., and Collins, W. D.: Radiative forcing by long-lived greenhouse gases: Calculations with the AER radiative transfer models, Journal of Geophysical Research: Atmospheres, 113, https://doi.org/10.1029/2008JD009944, 2008.

Intergovernmental Panel on Climate Change (IPCC): 2006 IPCC Guidelines for National Greenhouse Gas Inventories, https://www.ipcc-nggip.iges.or.jp/public/2006gl/index.html, 2006.

Kurokawa, J. and Ohara, T.: Long-term historical trends in air pollutant emissions in Asia: Regional Emission inventory in ASia (REAS) version 3, Atmospheric Chemistry and Physics, 20, 12 761–12 793, https://doi.org/10.5194/acp-20-12761-2020, 2020.

Lamarque, J. F., Bond, T. C., Eyring, V., Granier, C., Heil, A., Klimont, Z., Lee, D., Liousse, C., Mieville, A., Owen, B., Schultz, M. G., Shindell, D., Smith, S. J., Stehfest, E., Van Aardenne, J., Cooper, O. R., Kainuma, M., Mahowald, N., McConnell, J. R., Naik, V., Riahi, K., and Van Vuuren, D. P.: Historical (1850-2000) gridded anthropogenic and biomass burning emissions of reactive gases and aerosols: Methodology and application, https://doi.org/10.5194/acp-10-7017-2010, 2010.

Lee, K., Ko, J., and Jung, S.: Quantifying uncertainty in carbon emission estimation: Metrics and methodologies, Journal of Cleaner Production, 452, 142 141, https://doi.org/10.1016/j.jclepro.2024.142141, 2024.

https://doi.org/10.5194/egusphere-2025-268
Preprint. Discussion started: 26 March 2025

Li, C., Liu, Y., Cheng, B., Zhang, Y., Liu, X., Qu, Y., An, J., Kong, L., Zhang, Y., Zhang, C., Tan, Q., and Feng, M.: A comprehensive investigation on volatile organic compounds (VOCs) in 2018 in Beijing, China: Characteristics, sources and behaviours in response to O3 formation, Science of The Total Environment, 806, 150 247, https://doi.org/10.1016/j.scitotenv.2021.150247, 2022.

Li, M., Zhang, Q., Streets, D. G., He, K. B., Cheng, Y. F., Emmons, L. K., Huo, H., Kang, S. C., Lu, Z., Shao, M., Su, H., Yu, X., and Zhang, Y.: Mapping Asian anthropogenic emissions of non-methane volatile organic compounds to multiple chemical mechanisms, Atmospheric Chemistry and Physics, 14, 5617–5638, https://doi.org/10.5194/acp-14-5617-2014, 2014.

Li, M., Zhang, Q., Kurokawa, J. I., Woo, J. H., He, K., Lu, Z., Ohara, T., Song, Y., Streets, D. G., Carmichael, G. R., Cheng, Y., Hong, C., Huo, H., Jiang, X., Kang, S., Liu, F., Su, H., and Zheng, B.: MIX: A mosaic Asian anthropogenic emission inventory under the international collaboration framework of the MICS-Asia and HTAP, https://doi.org/10.5194/acp-17-935-2017, 2017.

Li, M., Zhang, Q., Zheng, B., Tong, D., Lei, Y., Liu, F., Hong, C., Kang, S., Yan, L., Zhang, Y., Bo, Y., Su, H., Cheng, Y., and He, K.: Persistent growth of anthropogenic non-methane volatile organic compound (NMVOC) emissions in China during 1990–2017: drivers, speciation and ozone formation potential, Atmospheric Chemistry and Physics, 19, 8897–8913, https://doi.org/10.5194/acp-19-8897-2019, 2019.

Li, M., Kurokawa, J., Zhang, Q., Woo, J.-H., Morikawa, T., Chatani, S., Lu, Z., Song, Y., Geng, G., Hu, H., Kim, J., Cooper, O. R., and McDonald, B. C.: MIXv2: a long-term mosaic emission inventory for Asia (2010–2017), Atmospheric Chemistry and Physics, 24, 3925–3952, https://doi.org/10.5194/acp-24-3925-2024, 2024a.

Li, M., Kurokawa, J., Zhang, Q., Woo, J.-H., Morikawa, T., Chatani, S., Lu, Z., Song, Y., Geng, G., Hu, H., Kim, J., Cooper, O. R., and McDonald, B. C.: MIXv2: a long-term mosaic emission inventory for Asia (2010–2017), Atmospheric Chemistry and Physics, 24, 3925–3952, https://doi.org/10.5194/acp-24-3925-2024, 2024b.

Liu, Y. and Wang, T.: Worsening urban ozone pollution in China from 2013 to 2017 - Part 2: The effects of emission changes and implications for multi-pollutant control, Atmospheric Chemistry and Physics, 20, 6323–6337, https://doi.org/10.5194/acp-20-6323-2020, 2020.

Lu, X., Zhang, L., Wang, X., Gao, M., Li, K., Zhang, Y., Yue, X., and Zhang, Y.: Rapid increases in warm-season surface ozone and resulting health impact in China since 2013, Environmental Science & Technology Letters, 7, 240–247, https://doi.org/10.1021/acs.estlett.0c00171, 2020.

Lv, D., Lu, S., He, S., Song, K., Shao, M., Xie, S., and Gong, Y.: Research on accounting and detection of volatile organic compounds from a typical petroleum refinery in Hebei, North China, Chemosphere, 281, 130 653, https://doi.org/10.1016/j.chemosphere.2021.130653, 2021.

Lyu, X., Li, K., Guo, H., Morawska, L., Zhou, B., Zeren, Y., Jiang, F., Chen, C., Goldstein, A. H., Xu, X., Wang, T., Lu, X., Zhu, T., Querol, X., Chatani, S., Latif, M. T., Schuch, D., Sinha, V., Kumar, P., Mullins, B., Seguel, R., Shao, M., Xue, L., Wang, N., Chen, J., Gao, J., Chai, F., Simpson, I., Sinha, B., and Blake, D. R.: A synergistic ozone-climate control to address emerging ozone pollution challenges, One Earth, 6, 964–977, https://doi.org/10.1016/j.oneear.2023.07.004, 2023.

McDonald, B. C., de Gouw, J. A., Gilman, J. B., Jathar, S. H., Akherati, A., Cappa, C. D., Jimenez, J. L., Lee-Taylor, J., Hayes, P. L., McKeen, S. A., Cui, Y. Y., Kim, S.-W., Gentner, D. R., Isaacman-VanWertz, G., Goldstein, A. H., Harley, R. A., Frost, G. J., Roberts, J. M., Ryerson, T. B., and Trainer, M.: Volatile chemical products emerging as largest petrochemical source of urban organic emissions, Science, 359, 760–764, https://doi.org/10.1126/science.aaq0524, 2018.

Mo, Z., Shao, M., and Lu, S.: Compilation of a source profile database for hydrocarbon and OVOC emissions in China, Atmospheric Environment, 143, 209–217, https://doi.org/10.1016/j.atmosenv.2016.08.025, 2016.

Monica, C.: HTAP_v3 emission mosaic, https://doi.org/10.5281/zenodo.7516361, https://doi.org/10.5281/zenodo.7516361, 2023.

Monks, P. S., Archibald, A. T., Colette, A., Cooper, O., Coyle, M., Derwent, R., Fowler, D., Granier, C., Law, K. S., Mills, G. E., Stevenson, D. S., Tarasova, O., Thouret, V., von Schneidemesser, E., Sommariva, R., Wild, O., and Williams, M. L.: Tropospheric ozone and its

https://doi.org/10.5194/egusphere-2025-268
Preprint. Discussion started: 26 March 2025

precursors from the urban to the global scale from air quality to short-lived climate forcer, Atmospheric Chemistry and Physics, 15, 8889–8973, https://doi.org/10.5194/acp-15-8889-2015, 2015.

Qu, K., Yan, Y., Wang, X., Jin, X., Vrekoussis, M., Kanakidou, M., Brasseur, G. P., Lin, T., Xiao, T., Cai, X., Zeng, L., and Zhang, Y.: The effect of cross-regional transport on ozone and particulate matter pollution in China: A review of methodology and current knowledge, Science of The Total Environment, p. 174196, https://doi.org/10.1016/j.scitotenv.2024.174196, 2024.

Rowlinson, M. J., Evans, M. J., Carpenter, L. J., Read, K. A., Punjabi, S., Adedeji, A., Fakes, L., Lewis, A., Richmond, B., Passant, N., Murrells, T., Henderson, B., Bates, K. H., and Helmig, D.: Revising VOC emissions speciation improves the simulation of global background ethane and propane, Atmospheric Chemistry and Physics, 24, 8317–8342, https://doi.org/10.5194/acp-24-8317-2024, 2024.

Sha, Q., Zhu, M., Huang, H., Wang, Y., Huang, Z., Zhang, X., Tang, M., Lu, M., Chen, C., Shi, B., Chen, Z., Wu, L., Zhong, Z., Li, C., Xu, Y., Yu, F., Jia, G., Liao, S., Cui, X., Liu, J., and Zheng, J.: A newly integrated dataset of volatile organic compounds (VOCs) source profiles and implications for the future development of VOCs profiles in China, Science of The Total Environment, 793, 148 348, https://doi.org/10.1016/j.scitotenv.2021.148348, 2021.

Skamarock, C., Klemp, B., Dudhia, J., Gill, O., Liu, Z., Berner, J., Wang, W., Powers, G., Duda, G., Barker, D. M., and Huang, X.: A Description of the Advanced Research WRF Model Version 4, https://api.semanticscholar.org/CorpusID:196211930, 2019.

Smith, S. J., McDuffie, E. E., and Charles, M.: Opinion: Coordinated development of emission inventories for climate forcers and air pollutants, Atmospheric Chemistry and Physics, 22, 13 201–13 218, https://doi.org/10.5194/acp-22-13201-2022, 2022.

Solazzo, E., Crippa, M., Guizzardi, D., Muntean, M., Choulga, M., and Janssens-Maenhout, G.: Uncertainties in the Emissions Database for Global Atmospheric Research (EDGAR) emission inventory of greenhouse gases, Atmospheric Chemistry and Physics, 21, 5655–5683, https://doi.org/10.5194/acp-21-5655-2021, 2021.

Song, M., Li, X., Yang, S., Yu, X., Zhou, S., Yang, Y., Chen, S., Dong, H., Liao, K., Chen, Q., Lu, K., Zhang, N., Cao, J., Zeng, L., and Zhang, Y.: Spatiotemporal variation, sources, and secondary transformation potential of volatile organic compounds in Xi'an, China, Atmospheric Chemistry and Physics, 21, 4939–4958, https://doi.org/10.5194/acp-21-4939-2021, https://acp.copernicus.org/articles/21/4939/2021/, 2021.

Soulie, A., Granier, C., Darras, S., Zilbermann, N., Doumbia, T., Guevara, M., Jalkanen, J.-P., Keita, S., Liousse, C., Crippa, M., Guizzardi, D., Hoesly, R., and Smith, S.: Global Anthropogenic Emissions (CAMS-GLOB-ANT) for the Copernicus Atmosphere Monitoring Service Simulations of Air Quality Forecasts and Reanalyses, Earth System Science Data Discussions, 2023, 1–45, https://doi.org/10.5194/essd-2023-306, 2023.

von Schneidemesser, E., McDonald, B. C., Denier van der Gon, H., Crippa, M., Guizzardi, D., Borbon, A., Dominutti, P., Huang, G., Jansens-Maenhout, G., Li, M., et al.: Comparing Urban Anthropogenic NMVOC Measurements with Representation in Emission Inventories-A Global Perspective, Journal of Geophysical Research: Atmospheres, p. e2022JD037906, https://doi.org/10.1029/2022JD037906, 2023.

Wang, W., Li, X., Cheng, Y., Parrish, D. D., Ni, R., Tan, Z., Liu, Y., Lu, S., Wu, Y., Chen, S., et al.: Ozone pollution mitigation strategy informed by long-term trends of atmospheric oxidation capacity, Nature Geoscience, 17, 20–25, https://doi.org/10.1038/s41561-023-01334-9, 2024.

Wang, Y., Li, W., Gao, W., Liu, Z., Tian, S., Shen, R., Ji, D., Wang, S., Wang, L., Tang, G., Song, T., Cheng, M., Wang, G., Gong, Z., Hao, J., and Zhang, Y.: Trends in particulate matter and its chemical compositions in China from 2013–2017, Science China Earth Sciences, 62, 1857–1871, https://doi.org/10.1007/s11430-018-9373-1, 2019.

Wang, Y., Zhao, Y., Liu, Y., Jiang, Y., Zheng, B., Xing, J., Liu, Y., Wang, S., and Nielsen, C. P.: Sustained emission reductions have restrained the ozone pollution over China, Nature Geoscience, pp. 1–8, https://doi.org/10.1038/s41561-023-01284-2, 2023.

https://doi.org/10.5194/egusphere-2025-268
Preprint. Discussion started: 26 March 2025

Wiedinmyer, C., Akagi, S. K., Yokelson, R. J., Emmons, L. K., Al-Saadi, J. A., Orlando, J. J., and Soja, A. J.: The Fire INventory from NCAR (FINN): a high resolution global model to estimate the emissions from open burning, Geoscientific Model Development, 4, 625–641, https://doi.org/10.5194/gmd-4-625-2011, 2011.

World Health Organization: Climate Change and Health, https://iris.who.int/bitstream/handle/10665/345329/9789240034228-eng.pdf?isAllowed=y&sequence=1, 2021.

WRF Model Development Team: WRF Model Releases, https://github.com/wrf-model/WRF/releases, accessed: March 17, 2025, 2025.

Wu, N., Geng, G., Xu, R., Liu, S., Liu, X., Shi, Q., Zhou, Y., Zhao, Y., Liu, H., Song, Y., Zheng, J., Zhang, Q., and He, K.: Development of a high-resolution integrated emission inventory of air pollutants for China, Earth System Science Data, 16, 2893–2915, https://doi.org/10.5194/essd-16-2893-2024, 2024.

Wu, R., Zhao, Y., Xia, S., Hu, W., Xie, F., Zhang, Y., Sun, J., Yu, H., An, J., and Wang, Y.: Reconciling the bottom-up methodology and ground measurement constraints to improve the city-scale NMVOCs emission inventory: A case study of Nanjing, China, Science of The Total Environment, 812, 152 447, https://doi.org/10.1016/j.scitotenv.2021.152447, 2022.

Yan, X., Xu, Y., and Pan, G.: Evolution of China's NOx emission control strategy during 2005â^¼2020 over coal-fired power plants: A satellite-based assessment, Journal of Environmental Management, 348, 119 243, https://doi.org/10.1016/j.jenvman.2023.119243, 2023.

Yin, P., Brauer, M., Cohen, A. J., Wang, H., Li, J., Burnett, R. T., Stanaway, J. D., Causey, K., Larson, S., Godwin, W., et al.: The effect of air pollution on deaths, disease burden, and life expectancy across China and its provinces, 1990–2017: an analysis for the Global Burden of Disease Study 2017, The Lancet Planetary Health, 4, e386–e398, https://doi.org/10.1016/j.apr.2022.101390, 2020.

Zhai, H., Huang, L., Emery, C., Zhang, X., Wang, Y., Yarwood, G., Fu, J. S., and Li, L.: Recommendations on benchmarks for photochemical air quality model applications in China — NO2, SO2, CO and PM10, Atmospheric Environment, 319, 120 290, https://doi.org/10.1016/j.atmosenv.2023.120290, 2024.

Zhang, K., Xu, J., Huang, Q., Zhou, L., Fu, Q., Duan, Y., and Xiu, G.: Precursors and potential sources of ground-level ozone in suburban Shanghai, Frontiers of Environmental Science and Engineering, 14, https://doi.org/10.1007/s11783-020-1271-8, 2020.

Zhang, Q., Zheng, Y., Tong, D., Shao, M., Wang, S., Zhang, Y., Xu, X., Wang, J., He, H., Liu, W., Ding, Y., Lei, Y., Li, J., Wang, Z., Zhang, X., Wang, Y., Cheng, J., Liu, Y., Shi, Q., Yan, L., Geng, G., Hong, C., Li, M., Liu, F., Zheng, B., Cao, J., Ding, A., Gao, J., Fu, Q., Huo, J., Liu, B., Liu, Z., Yang, F., He, K., and Hao, J.: Drivers of improved PM2.5 air quality in China from 2013 to 2017, https://doi.org/10.1073/pnas.1907956116, 2019.

Zhang, Y.: CINEI V1.1: Python code for creating an integrated inventory of anthropogenic emission for China (Version 1), https://doi.org/10.5281/zenodo.15000795, 2025a.

Zhang, Y.: Data used in manuscript 'Towards an integrated inventory of anthropogenic emissions for China' (submitted to Geoscientific Model Development journal), https://doi.org/10.5281/zenodo.15039737, https://doi.org/10.5281/zenodo.15039737, 2025b.

Zhang, Y., Xue, L., Carter, W. P., Pei, C., Chen, T., Mu, J., Wang, Y., Zhang, Q., and Wang, W.: Development of ozone reactivity scales for volatile organic compounds in a Chinese megacity, https://doi.org/10.5194/acp-21-11053-2021, 2021.

Zhang, Y., Vrekoussis, M., and Brasseur, G.: CINEI V1.1: Integrated Anthropogenic Emission Inventory for China [dataset], https://doi.org/10.1594/PANGAEA.974347, dataset in review, 2025.

Zhao, Y., Nielsen, C. P., McElroy, M. B., Zhang, L., and Zhang, J.: CO emissions in China: Uncertainties and implications of improved energy efficiency and emission control, Atmospheric Environment, 49, 103–113, https://doi.org/https://doi.org/10.1016/j.atmosenv.2011.12.015, https://www.sciencedirect.com/science/article/pii/S1352231011012672, 2012.

https://doi.org/10.5194/egusphere-2025-268
Preprint. Discussion started: 26 March 2025

Zheng, B., Tong, D., Li, M., Liu, F., Hong, C., Geng, G., Li, H., Li, X., Peng, L., Qi, J., Yan, L., Zhang, Y., Zhao, H., Zheng, Y., He, K., and Zhang, Q.: Trends in China's anthropogenic emissions since 2010 as the consequence of clean air actions, Atmospheric Chemistry and Physics, 18, 14 095–14 111, https://doi.org/10.5194/acp-18-14095-2018, 2018.

Zheng, B., Zhang, Q., Geng, G., Chen, C., Shi, Q., Cui, M., Lei, Y., and He, K.: Changes in China's anthropogenic emissions and air quality during the COVID-19 pandemic in 2020, https://doi.org/10.5194/essd-13-2895-2021, 2021a.

Zheng, Y., Jiang, F., Feng, S., Cai, Z., Shen, Y., Ying, C., Wang, X., and Liu, Q.: Long-range transport of ozone across the eastern China seas: A case study in coastal cities in southeastern China, Science of The Total Environment, 768, 144 520, https://doi.org/https://doi.org/10.1016/j.scitotenv.2020.144520, https://www.sciencedirect.com/science/article/pii/S0048969720380517, 2021b.